

## **A Method to Study the Correlation Between Local Collagen Structure and Mechanical Properties of Atherosclerotic Plaque Fibrous Tissue**

Crielaard, Hanneke; Guvenir Torun, Su; Wissing, Tamar B.; de Miguel Muñoz, Pablo; Kremers, Gert Jan; Gijzen, Frank J.H.; Van Der Heiden, Kim; Akyildiz, Ali C.

**DOI**

[10.3791/64334](https://doi.org/10.3791/64334)

**Publication date**

2022

**Document Version**

Final published version

**Published in**

Journal of visualized experiments : JoVE

**Citation (APA)**

Crielaard, H., Guvenir Torun, S., Wissing, T. B., de Miguel Muñoz, P., Kremers, G. J., Gijzen, F. J. H., Van Der Heiden, K., & Akyildiz, A. C. (2022). A Method to Study the Correlation Between Local Collagen Structure and Mechanical Properties of Atherosclerotic Plaque Fibrous Tissue. *Journal of visualized experiments : JoVE*, 2022(189), Article e64334. <https://doi.org/10.3791/64334>

**Important note**

To cite this publication, please use the final published version (if applicable).  
Please check the document version above.

**Copyright**

Other than for strictly personal use, it is not permitted to download, forward or distribute the text or part of it, without the consent of the author(s) and/or copyright holder(s), unless the work is under an open content license such as Creative Commons.

**Takedown policy**

Please contact us and provide details if you believe this document breaches copyrights.  
We will remove access to the work immediately and investigate your claim.

# A Method to Study the Correlation Between Local Collagen Structure and Mechanical Properties of Atherosclerotic Plaque Fibrous Tissue

Hanneke Crielaard<sup>1</sup>, Su Guvenir Torun<sup>1</sup>, Tamar B. Wissing<sup>1,2</sup>, Pablo de Miguel Muñoz<sup>1,3</sup>, Gert-Jan Kremers<sup>4</sup>, Frank J. H. Gijzen<sup>1,3</sup>, Kim Van Der Heiden<sup>1,2</sup>, Ali C. Akyildiz<sup>1,3</sup>

<sup>1</sup> Department of Biomedical Engineering, Erasmus Medical Center <sup>2</sup> Department of Biomedical Engineering, Eindhoven University of Technology <sup>3</sup> Department of Biomechanical Engineering, Delft University of Technology <sup>4</sup> Erasmus Optical Imaging Center, Erasmus Medical Center

## Corresponding Author

Hanneke Crielaard

[h.crielaard@erasmusmc.nl](mailto:h.crielaard@erasmusmc.nl)

## Citation

Crielaard, H., Guvenir Torun, S., Wissing, T.B., de Miguel Muñoz, P., Kremers, G.J., Gijzen, F.J.H., Van Der Heiden, K., Akyildiz, A.C. A Method to Study the Correlation Between Local Collagen Structure and Mechanical Properties of Atherosclerotic Plaque Fibrous Tissue. *J. Vis. Exp.* (189), e64334, doi:10.3791/64334 (2022).

## Date Published

November 11, 2022

## DOI

10.3791/64334

## URL

[jove.com/video/64334](https://jove.com/video/64334)

## Abstract

The rupture of atherosclerotic plaques in coronary and carotid arteries is the primary cause of fatal cardiovascular events. However, the rupture mechanics of the heterogeneous, highly collagenous plaque tissue, and how this is related to the tissue's fibrous structure, are not known yet. Existing pipelines to study plaque mechanics are limited to obtaining only gross mechanical characteristics of the plaque tissue, based on the assumption of structural homogeneity of the tissue. However, fibrous plaque tissue is structurally heterogeneous, arguably mainly due to local variation in the collagen fiber architecture.

The mechano-imaging pipeline described here has been developed to study the heterogeneous structural and mechanical plaque properties. In this pipeline, the tissue's local collagen architecture is characterized using multiphoton microscopy (MPM) with second-harmonic generation (SHG), and the tissue's failure behavior is characterized under uniaxial tensile testing conditions using digital image correlation (DIC) analysis. This experimental pipeline enables correlation of the local predominant angle and dispersion of collagen fiber orientation, the rupture behavior, and the strain fingerprints of the fibrous plaque tissue. The obtained knowledge is key to better understand, predict, and prevent atherosclerotic plaque rupture events.

## Introduction

Ischemic stroke, often triggered by atherosclerotic plaque rupture in carotid arteries, is one of the leading causes of mortality and morbidity worldwide<sup>1</sup>. However, the current surgical treatment planning strategies to prevent carotid

atherosclerosis-related stroke do not include plaque rupture risk assessment<sup>2</sup>. This is mainly because the previously suggested risk biomarkers, such as plaque cap thickness<sup>3</sup> and lipid core size<sup>4</sup>, have been shown to have suboptimal

predictive value for future clinical events<sup>5,6</sup>. A better understanding of plaque mechanics and rupture mechanisms is necessary to optimize plaque rupture risk assessment and identify new risk markers of atherosclerotic plaques.

Plaque rupture is a local mechanical event where the highly fibrous plaque tissue fails to withstand the mechanical loading exerted on it by the blood pressure and loses its structural integrity<sup>7</sup>. Despite this, the mechanics of the plaque rupture event and its link to the underlying microstructure are poorly understood<sup>8</sup>. The few experimental studies that characterized plaque tissue failure features<sup>9,10,11,12,13</sup> reported gross mechanical rupture properties (i.e., ultimate tensile failure strain and strength), derived with the assumption of structural homogeneity of the tissue. However, the fibrous plaque tissue is structurally heterogeneous, arguably mainly due to local variation in the collagen fiber architecture<sup>14</sup>. Moreover, the link between the plaque tissue mechanical failure characteristics and the collagen architecture was only investigated in a recent study by Johnston et al. The authors showed an interplaque difference in the predominant fiber orientation and reported higher ultimate stresses and lower ultimate strains for fibrous plaque cap samples with a predominantly circumferential fiber orientation<sup>15</sup>. However, the study was also limited to gross mechanical and structural properties.

To shed light on the essential information about the local collagen architecture and local mechanical properties of the fibrous plaque tissue, in the current study, we have developed a mechano-imaging pipeline. This *ex vivo* pipeline enables quantification of the local collagen fiber direction and dispersion, as well as local rupture strain. The pipeline involves MPM imaging with SHG to image collagen fibers in

the plaque tissue, as well as DIC and uniaxial tensile testing to quantify the tissue's rupture characteristics.

Multiphoton microscopy-second-harmonic generation (MPM-SHG) has become a popular technique to study collagen in biological tissues<sup>16</sup>. The technique has many advantages compared to other collagen imaging techniques, such as histology<sup>17</sup>, diffusion tensor imaging (DTI)<sup>14</sup>, and small-angle light scattering (SALS)<sup>15</sup>. First, MPM-SHG imaging is non-destructive, which makes it ideal to combine with mechanical testing<sup>18</sup>. Second, the SHG signal is specific for collagen, and therefore no staining of the tissue is necessary. Due to the long excitation wavelengths (near-infrared), the penetration depth is greater than with other microscopy techniques<sup>16</sup>. The high resolution ( $\mu\text{m}$ -level) achieved with SHG imaging also allows visualization of individual fibers. This offers many possibilities, such as local quantification of the number of collagen fibers, collagen fiber orientation, and distribution<sup>19</sup>.

Digital image correlation (DIC) combined with mechanical testing is a widely used method to obtain local mechanical properties of biological tissues<sup>20</sup>. With DIC, the displacement of speckles applied on the tissue surface is tracked by comparing high-speed camera images acquired during mechanical testing<sup>20</sup>. This image postprocessing method is used to estimate the full-field surface strains of the specimen<sup>20</sup> and can also be used to study the rupture behavior of the tissue<sup>21</sup>.

## Protocol

All methods described in this paper were approved by the Ethical Research Committee at the Erasmus Medical Center in Rotterdam; informed consent was obtained from patients before plaque specimen collection. A workflow chart of the protocol is given in **Figure 1**.

## 1. Tissue collection, micro-computed tomography ( $\mu$ CT) imaging, and test sample preparation

### 1. Tissue collection and storage

1. Collect fresh human carotid atherosclerotic plaque specimens from consenting patients who underwent carotid endarterectomy surgery.

**NOTE:** The plaque samples retrieved from this surgery consist of the diseased intima layer of the carotid artery, including the accumulation of fat (the lipid pool) and calcifications<sup>22</sup>.

2. Remove blood remnants using phosphate-buffered saline (1x PBS) and dry the specimen with a gauze pad.
3. Place the specimen in a 15 mL tube using tweezers. Snap-freeze the tissue by placing the tube in liquid nitrogen for 10 min.
4. After snap-freezing, store the sample in a  $-80\text{ }^{\circ}\text{C}$  freezer until the day of  $\mu$ CT imaging.

**NOTE:** Snap-freezing minimizes crystal formation, leading to microstructural damage in the tissue. A previous study on porcine aortic tissue has shown that snap-freezing and storage at  $-80\text{ }^{\circ}\text{C}$  had no significant influence on the tissue's mechanical properties<sup>23</sup>.

### 2. $\mu$ CT imaging

1. On the day of  $\mu$ CT imaging, take the plaque specimen out of the 15 mL tube. If the tissue sticks to the tube, fill the tube with PBS at room temperature. Leave the tissue in PBS until the sample can be taken out of the tube.
2. Dry the plaque specimen thoroughly with tissue paper.

3. Turn on the  $\mu$ CT system by pressing the **green** button. Press **warm up** in the CT software at the bottom of the screen and wait 15 min.
4. Manually place an X-ray filter of Cu 0.06 mm + Al 0.5 mm in the  $\mu$ CT system.
5. Select the folder in which the images are to be stored.
6. Choose the parameters in the **left panel**. Use the dropdown lists to select a **scanning time** of **4 min**, a **resolution** of **172  $\mu\text{m}$** , a **voltage** of **90 kV**, an **amperage** of **88 mA**, a **field of view** of **86 mm**, and a **rotation** of **360 $^{\circ}$** .
7. Open the door of the device. Pull the platform out manually.
8. Put parafilm on the platform and place the sample on the platform (toward the further extreme of the platform).
9. Manually place the platform into the device and close the door.
10. Activate the **live mode** (**eye** icon). Move the platform with the arrows in the device to center the sample in the FOV.
11. **Start** imaging (icon in the bottom-middle). Once the imaging is finished, press the **door** icon at the bottom (under the **abort** button).
12. After the  $\mu$ CT scan, snap-freeze the plaque specimen again as described in step 1.1.3. Store it at  $-80\text{ }^{\circ}\text{C}$  until the day of multiphoton microscopy imaging and mechanical testing.
13. Open the acquired DICOM files of the  $\mu$ CT imaging in the open-source 3D Slicer software<sup>24</sup>.

14. Go to **Segment** editor. Select **create a new segmentation | the volume to be analyzed as a master volume**.
15. Click on **Add** to add a segment. Press its **name** and **color** to change these **parameters**.
16. To define the segments, click on **effects | threshold** in the bottom part of the window. Use this **threshold** tool to differentiate between **calcified (>450 HU)** and **non-calcified (<450 HU)** tissue regions. Once the threshold is selected, press **Apply** in the bottom part.
17. Press **Show 3D** (just to the right of **Add**) to visualize the segmentation in the 3D view. If there are areas of the segmentation that are not desired, remove them with the **scissors** effect.
18. Change the opacity of segments in the **segmentation** module by clicking on the **name of the desired segmentation**.

**NOTE:** If possible,  $\mu$ CT imaging and reviewing of the  $\mu$ CT images can be performed on the same day as the rest of the protocol. In that case, skip step 1.2.12. However, take into account that the subsequent steps of this protocol are also time-consuming and should be performed on the same day. After some practice, and with the described settings and tissue,  $\mu$ CT imaging should take ~45 min, reviewing of the  $\mu$ CT images ~15 min, test sample preparation of a single test sample ~1 h, microscopy ~4 h, and uniaxial tensile testing ~2 h.

### 3. Test sample preparation

1. On the day of collagen imaging and mechanical testing, thaw the plaque by submersion in PBS at room temperature for approximately 10 min.

2. Open the 3D construction of the plaque created in steps 1.2.13-1.2.18 in the 3D slicer software.
3. Use the natural landmarks of the plaque tissue to identify which parts of the 3D reconstruction correspond to the real plaque sample. Identify which area of the 3D reconstruction does not contain calcifications and visually identify this area in the real plaque.
4. Cut the plaque open along the longitudinal axis of the artery using surgical scissors and tweezers. If a cut is already present from the surgery, start from this cut for optimal usage of the tissue. If the sample does not have a tubular shape and it is difficult to define the longitudinal direction, exclude the sample from testing.
5. Cut out rectangular test samples from the plaque specimens. Make sure the test samples are as large as possible while avoiding tissue regions containing tears or calcifications. Be careful during this cutting, as a small tear or crack at the edge of the test specimen can result in crack-propagation from the existing crack during tensile testing.
6. Make sure that the test samples have a width-to-length (WL) ratio of  $<1$  in the gauge length once mounted in the tensile tester. If the samples meet this requirement, they are suitable for appropriate tensile tests in terms of boundary conditions<sup>25</sup>.

**NOTE:** The range in the sample dimensions can be large. The samples that the authors tested had a gauge length that ranged between 3.4 and 12.9 mm and a width that ranged between 1.6 and 6.4 mm.

## 2. Multiphoton microscopy imaging

### 1. Preparations

1. Before the day of collagen imaging and mechanical testing, divide 40 g of a silicone elastomer base over two 50 mL tubes and add 2 g of the curing agent to each tube (ratio of 1:10) using a Pasteur pipet. Mix the two components with the pipet.
2. Centrifuge the tubes for 1 min at  $700 \times g$  to remove as many air bubbles as possible.
3. Fill a Petri dish (10 cm diameter) with a thin layer (approximately 0.5-1 cm) of silicon and either incubate it in the oven at  $65^\circ\text{C}$  for 3 h or place it at room temperature for 48 h.
4. Take a plaque test sample and fix both its ends to the silicon by pinning needles in the tissue (**Figure 2A**). Make sure the luminal side of the sample is facing upward. Insert the needles in the region of the sample that will be in the clamps of the tensile testing device during the mechanical testing.
5. Put on safety glasses. Use a side cutter to shorten the needles so that they stick out less than a few millimeters above the sample surface, to prevent them from damaging the microscope objective. Fill the Petri dish with PBS until the sample is submerged.

### 2. Microscopy setup

1. Make sure that a proper objective is mounted on the multiphoton microscope. Use an objective optimized to transmit infrared light, with a magnification of 20x.
2. Start up the microscope system. Open the operating software of the microscope.

3. When asked to initialize the imaging table, make sure the microscope condenser arm is pushed back and the objective is at the lowest position.
4. Activate the multiphoton laser.
5. Put the Petri dish with the test sample in it underneath the objective, as in **Figure 3**. Be sure not to place the objective above the sample yet as the laser settings still need to be optimized. Otherwise, the possible high power of the laser light may lead to damage to the tissue.
6. Make sure that the objective is slightly immersed in PBS. Use a pipet to add extra PBS if needed.
7. Set the light wavelength to 880 nm.

**NOTE:** This wavelength is chosen because the SHG emission filter in the used two-photon system has a center wavelength of approximately 440 nm. For other microscopes, a different wavelength might be more applicable.

### 3. Tile scan and selection of imaging locations

1. Turn off the multiphoton laser and activate the **brightfield** mode of the microscope. Then, turn on the **live scan** mode.
2. Position the stage such that the objective is located above the sample and bring the sample surface into focus. Turn **off** the **live scan** mode.
3. Under the **acquisition** tab, in the **second panel**, change the **zoom factor** to **1** by sliding the intended bar.

**NOTE:** This zoom factor, together with the magnification factor of the objective (20x), determine the size of the captured image ( $739 \mu\text{m} \times 739 \mu\text{m}$ ).

4. Under the **acquisition** tab, in the **second panel**, change the **scan speed** to **400 Hz**, the **line average** to **1**, and the **resolution** to **128 x 128 pixels per image (pixel size of ~5.8 μm x 5.8 μm)** by using the dropdown lists.
5. Under the **acquisition** tab, in the **first panel**, click the **raster pattern** symbol and wait for a **tile scan panel** to appear.
6. Turn on the **live scan** mode. Move the objective to a corner of the sample using the knobs on the smart panel and click the mark position symbol in the tile scan panel. Repeat this for each corner of the sample. If performed correctly, a grid with all selected tiles for imaging will appear in orange.
7. Toggle off the **auto-stitching** function.
8. Click **start** in the bottom-right corner of the screen to create a tile scan of the entire sample surface to obtain an overview of the sample geometry.  
**NOTE:** Based on the described settings, tissue, and microscope system, acquiring a tile scan of the entire sample surface takes ~10 min.
9. After the tile scan, observe the x- and y-coordinates of the upper left corner of each tile in the tile scan panel, shown automatically by the software of the microscopy system. Note these coordinates in a spreadsheet.
10. In the microscope software, in the **tile scan panel**, observe the number of tiles in the x- and y- directions in the box called **scanfield**. Note the size of the tile scan in the spreadsheet. Calculate the coordinates of the other tiles by adding/subtracting the size of the tile (739 μm).

**NOTE:** These coordinates are necessary to identify the exact location of the tiles to be scanned with SHG imaging. If the total imaging time is not a concern, all tiles can be imaged without skipping any tile.

11. From the tile scan, select the tiles to be imaged with SHG imaging. For this selection, avoid tiles that will be in the clamps and leave one tile between each selected tile in both the longitudinal and the circumferential direction, as shown in **Figure 2B**.
4. Visualizing collagen: SHG imaging
    1. Turn off the lights in the room and cover the microscope stage with blackout fabric also that no light from the room reaches the detector.  
**NOTE:** Minimizing light reaching the detectors will decrease the noise during image acquisition.
    2. Turn the **multiphoton (MP) laser** on.
    3. Select the **non-descanned detection (NDD) detector** that is equipped with a **430-450 nm bandpass filter**.
    4. Identify the location of the tiles to be imaged by using the information acquired in step 2.3.10. Fill in the **coordinates** in the designated boxes and click **enter**, so the objective moves to the right tile. Turn on the **live scan mode**.  
**NOTE:** With other microscopes or newer versions of the operating software, moving to locations within the tile scan can be done automatically. In this case, noting the x- and y- coordinates of each tile (step 2.3.10) and filling in the coordinates in the operating software (step 2.4.4) is not necessary.
    5. Increase the MP laser power by using the slider in the **upper panel** under **beam path settings** to get the highest possible laser power without

significant bleaching. Then, adjust the **detector gain** to obtain bright images, but without saturated pixels, by using the **knob** on the **smart panel** or by clicking on the name of the **detector** under **beam path settings | additional channels**. Typical values for the **detector gain** are between **500** and **800 V**.

6. Use the **z-position knob** on the **smart panel** to adjust the focus plane.
7. Move to the top of the sample and set the positions of the top of the z-stack by clicking on the **arrowhead** in the **z-stack panel** (under the **acquisition tab | 3<sup>rd</sup> panel**).
8. Then, focus on the sample until the SHG signal is no longer detected-this is the end of the stack. Again, click on the **arrowhead** in the **z-stack panel** to set this position. When finished, turn **off** the **live scan** mode.
 

**NOTE:** The tissue may not be entirely flat. Therefore, the sample surface of different regions within the tissue may have slightly different positions in the z-direction.
9. Under the **acquisition** tab, in the **second panel**, keep the **scan speed** at **400 Hz**, set the **line average** to **2**, and the **resolution** to **512 x 512 pixels per image (pixel size of ~1.4 μm x 1.4 μm)** by using the dropdown lists. Toggle on the **bidirectional X scanning button**.
10. Click on **z-step size** in the **z-stack panel** and fill a **z-step size** of **3 μm** in the box. Click **start** in the **bottom-right corner** of the screen to create a z-stack. When finished, be sure to save the coordinates of the tile in the file name or give each tile its own number (as in **Figure 2B**).

**NOTE:** Based on the described settings, tissue, and microscope system, the acquirement of a z-stack of a single tile takes ~10-15 min. The preparation steps (steps 2.4.4-2.4.10) are included within this time estimate.

### 3. Mechanical testing

1. Preparation of uniaxial tensile testing setup
  1. Make the horizontal tensile testing setup (**Figure 4**) ready for usage, following the instructions for the tensile tester (e.g., turn on software, attach clamps, attach load cell).
  2. To minimize the slippage of the test sample, attach two-sided foam tape (**Figure 4A,B-2**) to the inner faces of the clamps of the tensile tester and sandpaper to the inner side of the foam tape. Eventually, the sandpaper will be in contact with the test sample.
  3. Place the heating bath (**Figure 4A,B-3**) in position. Fill the heating bath with PBS up to the level of the bottom face of the clamps, so that it does not reach the sandpaper yet.
  4. Turn the power source of the heating bath on and set the temperature to around 37 °C.
  5. Mount the high-speed camera above the tensile testing system (**Figure 4A-4**), for example, by using a laboratory stand, and mount a lens with a focal length of 50 mm on the camera through an extension ring.
  6. Make sure that the clamps are in focus and that the field of view is large enough to record the sample during the entire stretching procedure (FOV width:



± the sample width; FOV length: ± 2x the sample length).

7. Mount the lighting system (**Figure 4A-5**) above the tensile testing system, for example, by using a laboratory stand. Turn the lighting system on and adjust the light intensity and location so that there are no reflections on the PBS surface to be observed on the camera image.
8. Adjust the **exposure time** and **gain** of the camera to obtain clear images.
9. Set the image acquisition software to capture at **30 frames/s** at a **resolution of 5.2 MP**.  
**NOTE:** This high frame rate is needed to perform the subsequent DIC analysis and study the rupture behavior.
10. Set the displacement speed of one of the clamps such that the global engineering strain rate during mechanical testing is similar to the *in vivo* physiological straining rate of the tissue (5%/s for plaque tissue<sup>26</sup>).

## 2. Generation of speckle pattern

**NOTE:** This speckle pattern protocol is based on previous work by Walsh et al.<sup>27</sup>.

1. Dry the sample by lightly dabbing it with tissue paper.
2. Put the black tissue dye in the intended bucket of the airbrush.
3. Connect the airbrush to the compressor. Turn the **airbrush compressor** on and set the **pressure to 25 PSI**.
4. Try creating an optimal speckle pattern on paper before spraying on the tissue. Spray a few times until a **black/white** ratio of **50:50**<sup>28</sup> is met. Move the

needle of the airbrush back and forth to adjust the roughness of the speckle pattern until the **size of a speckle** is similar to the size of **3-5 pixels** of the high-speed camera<sup>29</sup>.

**NOTE:** The speckle pattern will be used for two different purposes. First, the displacement of these speckles is measured by comparing high-speed camera images acquired during mechanical testing (DIC, step 4.2). Second, this speckle pattern is used to identify the rupture location on the image of the undeformed state of the sample (step 4.3.1).

5. Hold the airbrush approximately 30 cm away from the test sample and spray on the luminal surface.
6. Let the dye bond to the sample for 1 min at room temperature before submerging the sample in PBS.

## 3. Uniaxial tensile testing

1. Place the sample in the clamps of the tensile tester, with the circumferential direction of the samples aligned with the tensile stretching direction and the luminal side of the sample facing upward. Make sure the initial gauge length is set such that the **WL ratio** of the **strips** is **<1**.
2. Tighten the screws of the grips by applying a **torque** of **20 cNm** using a torque screwdriver. Do this gradually by applying a small torque to each screw before applying the final torque.
3. Visually inspect if the sample contains any tears that could influence the tests.
4. Introduce more PBS into the heating bath until the sample is submerged and wait until the temperature of the PBS has reached 37 °C again.

5. Acquire a calibration image with the high-speed camera, in which the test sample and a ruler are included as a reference. Make sure the ruler is at the same distance from the camera objective as the luminal surface of the sample.
6. Tare the load cell and start recording the global force and displacement measurements from the load cell and the actuator of the tensile tester.
7. Straighten the sample by applying a **prestretch** of **0.05 N** to get rid of the slack in the sample. Perform **10 cycles** of preconditioning up to **10% strain** based on the gauge length measurement by the actuator after the application of prestretch.
8. Start the uniaxial tensile testing until complete failure of the sample, while recording a video of the sample deformation with the high-speed camera. After tissue failure, stop recording the global force and displacement measurements.  
**NOTE:** Some commercial tensile testers can perform steps 3.3.6-3.3.9 automatically. The current protocol describes the manual steps to be taken if this automatic option is not included in the tensile tester being used.
9. Remove the test sample from the tensile testing device and discard it appropriately.
10. When testing the next sample, replace the sandpaper and foam tape on the clamps.

#### 4. Data analysis

##### 1. Collagen organization analysis

1. Open the z-stacks obtained during MPM with SHG in ImageJ and create maximum intensity projections (MIPs) of each z-stack.

2. Analyze each MIP with the open-source MATLAB-based FOA (Fiber Orientation Analysis) tool<sup>30</sup> to measure the orientation angle of the individual collagen fibers present in the tiles. Use the following parameters: **Scales: [3 4 5]** or **[2 4 6]**, depending on the vessel diameter, and **Vesselness threshold: 0.999, 0.9995, or 0.9999**, depending on the intensity of the SHG signal.

**NOTE:** More details about how to use this tool can be found in the software's manual<sup>31</sup>.

3. Use another open-source MATLAB-based tool, FibLab<sup>32</sup>, to fit a Gaussian distribution to the angle distribution histogram.

**NOTE:** More details about how to use this tool can be found in the software's manual<sup>32</sup>.

4. From the Gaussian distribution plot obtained using FibLab, extract the following structural parameters from the workspace of MATLAB: the **predominant fiber angle ( $\mu_p$ )**, which is the mode of the distribution, the **standard deviation ( $\sigma_p$ ) of the fiber angle distribution**, and the **anisotropic fraction ( $P_{ani} = 1 - P_{iso}$ )**.

**NOTE:** The isotropic fraction is the area under the baseline in the Gaussian distribution, while the anisotropic fraction contains the area of the peak on top of that baseline<sup>33</sup>. Both  $\sigma_p$  and  $P_{ani}$  provide information about the dispersion of the fibers' orientation in the tile region.

5. For visual inspection, plot  $\mu_p$  by using oriented lines and  $\sigma_p$  and  $P_{ani}$  by using color maps.

##### 2. Digital image analysis and rupture analysis

1. Perform visual inspection on the camera images to identify the frame in which rupture initiation occurs. On this frame, visually identify the rupture location.
2. Perform visual inspection on the camera images to identify any eventual crack or tear at the location of rupture at the start of mechanical testing. If such a tear is present, exclude the sample from analysis.
3. Perform the DIC analysis with the open-source, MATLAB-based software Ncorr (v1.2)<sup>34</sup>. Follow the steps in the Ncorr manual<sup>35</sup>.
  1. Use the camera images recorded during the tensile test with the high-speed camera for DIC. Select the last frame before the final stretching until failure (after preconditioning) as the **reference image**. For the **current images**, select all images from the start of the final stretching until the last frame before the frame in which rupture initiation occurred.
  2. Select the sample surface as the region of interest (ROI). Exclude the areas that are near (approximately 1 mm) to the clamps, as the strains in these areas will be highly influenced by the grips.
  3. Perform DIC analysis by using the following parameters: **Subset radius: 30 pixels; Subset spacing: three pixels; Iteration cutoff: 50; Norm of the difference vector cutoff: 10-5; Strain radius: 5; Auto propagation, step#: 5.**
  4. From the DIC analysis with Ncorr, obtain the Green-Lagrange (or Eulerian strain) distributions of the ROI. Use these strain distributions to calculate the average Green-

Lagrange strain of the entire plaque sample surface at the last frame before rupture. Calculate the Green-Lagrange strain at the rupture location.

3. Correlating structural and mechanical data at the rupture location
  1. Using the natural landmarks in the test sample and the applied speckles on the test sample, identify the rupture location (identified in step 4.2.1) on the reference image (step 4.2.3.1).
  2. Using the natural landmarks in the test sample, make an overlay of the reference image and the tile scan (step 2.3) to identify the rupture location on the tile scan. Identify the MPM-SHG tile where the rupture happened. If the rupture is not in a tile scanned with the MPM-SHG, identify the tile closest to the rupture location. Obtain the structural parameters found at the tile where rupture occurred.

## Representative Results

### Tissue collection and test sample preparation

The tissue collection yields plaque fibrous tissue specimens that can be dissected into individual test samples for structural imaging and uniaxial tensile testing. Ideally, a collected fibrous tissue sample contains areas with little to no tears (**Figure 5A**) and macrocalcifications (**Figure 5B**). An excess of these tears and calcifications (**Figure 5C**) may lead to plaque samples that do not meet the previously mentioned sample dimension requirement of WL 1.

### Multiphoton microscopy imaging

SHG imaging and image postprocessing provides MIPs from each imaged tile (**Figure 6A,B**). Further post-processing by fiber detection (**Figure 6C**) yields fiber orientation histograms

(**Figure 6D**) from which collagen structural parameters can be extracted (**Figure 6E**). In addition, color maps showing the local structural collagen parameters across the entire plaque sample can be obtained for visual analysis (**Figure 6F,G**). For the representative test sample in **Figure 6**, a large intrasample variation in the structural collagen parameters is found (average  $\pm$  SD of  $\mu_p = -34^\circ \pm 32^\circ$ ;  $\sigma_p = 21^\circ \pm 4^\circ$ ;  $P_{ani} = 0.49 \pm 0.14$ , if the circumferential direction is defined as  $0^\circ$ ). This intrasample variation emphasizes the importance of obtaining local structural parameters instead of assuming homogeneity.

## Mechanical testing

### Rupture behavior

The high-speed camera provides images of the deformation and rupture behavior of the plaque samples during mechanical testing (**Figure 7**). From these images, the location of rupture initiation and the rupture propagation path can be identified. The rupture identification results are suboptimal if bubbles or reflections are present in the camera images, or if the rupture propagates too fast to be captured by the chosen frame rate.

### Local strain patterns

Digital image correlation analysis on the camera recordings acquired during the uniaxial tensile testing provides the local tissue deformation maps, such as the Green-Lagrange strain maps shown in **Figure 8**. These maps display the three strain components ( $\epsilon_{xx}$ ,  $\epsilon_{xy}$ , and  $\epsilon_{yy}$ ) at the frame before rupture initiation. From these strain maps, the average strains in a

region of interest and local strain at a spot, such as rupture location, can be extracted.

For the representative sample in **Figure 8**, the local strain data show a large intrasample variation. For the representative test sample in **Figure 8**, a large intrasample variation in the local strains is found (the ranges of the observed strains are as follows:  $\epsilon_{xx} = -0.30-0.17$ ;  $\epsilon_{xy} = -0.13-0.20$ ;  $\epsilon_{yy} = 0-0.40$ ). This emphasizes the importance of obtaining local data instead of gross, average values obtained with the assumption of tissue homogeneity.

## Correlating mechanical and structural tissue information

The above-mentioned results allows association of the local deformation and rupture behavior of the tissue to the collagen architecture. Once the rupture location is identified on the camera recordings (**Figure 9A**), it can be mapped back to the reference camera image (**Figure 9B**) and to the microscopy tile scan (**Figure 9C**). This provides the MPM-SHG tile where the rupture happened and the structural parameters found at this tile (**Figure 9D**). The structural parameters found in the tile where rupture occurred in a representative sample, shown in **Figure 9**, are  $\mu_p = 28^\circ$ ,  $\sigma_p = 19^\circ$ , and  $P_{ani} = 0.6$ . The same procedure can also be applied to the non-ruptured tissue locations. It is important to note that mapping the rupture location on the reference image from the rupture frame may be challenging in case of a poor speckle pattern and unclear natural landmarks. In addition, if the natural landmarks of the tissue are not clear enough, co-registration of the tile scan overlay and the high-speed camera images may be difficult.

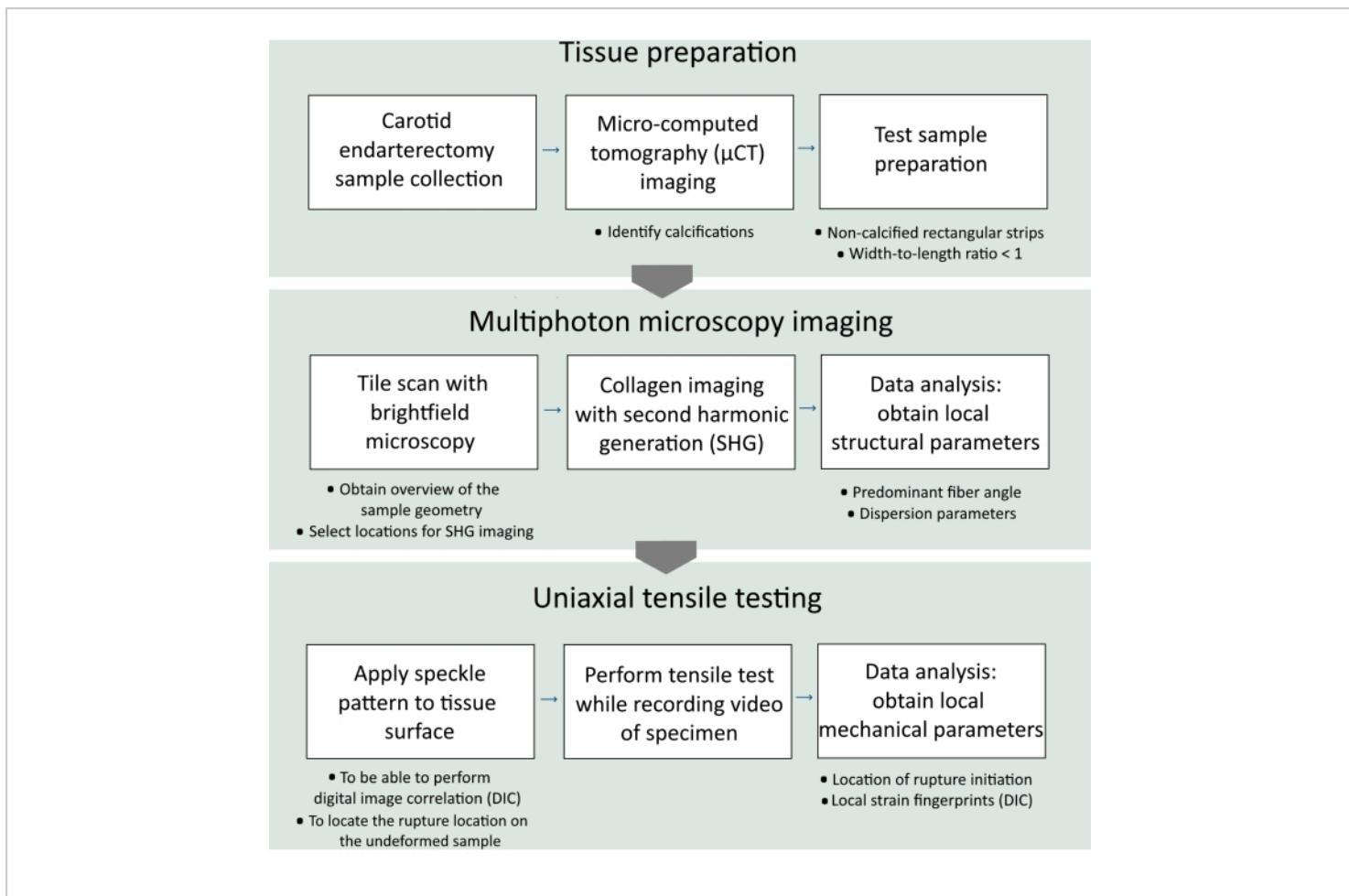
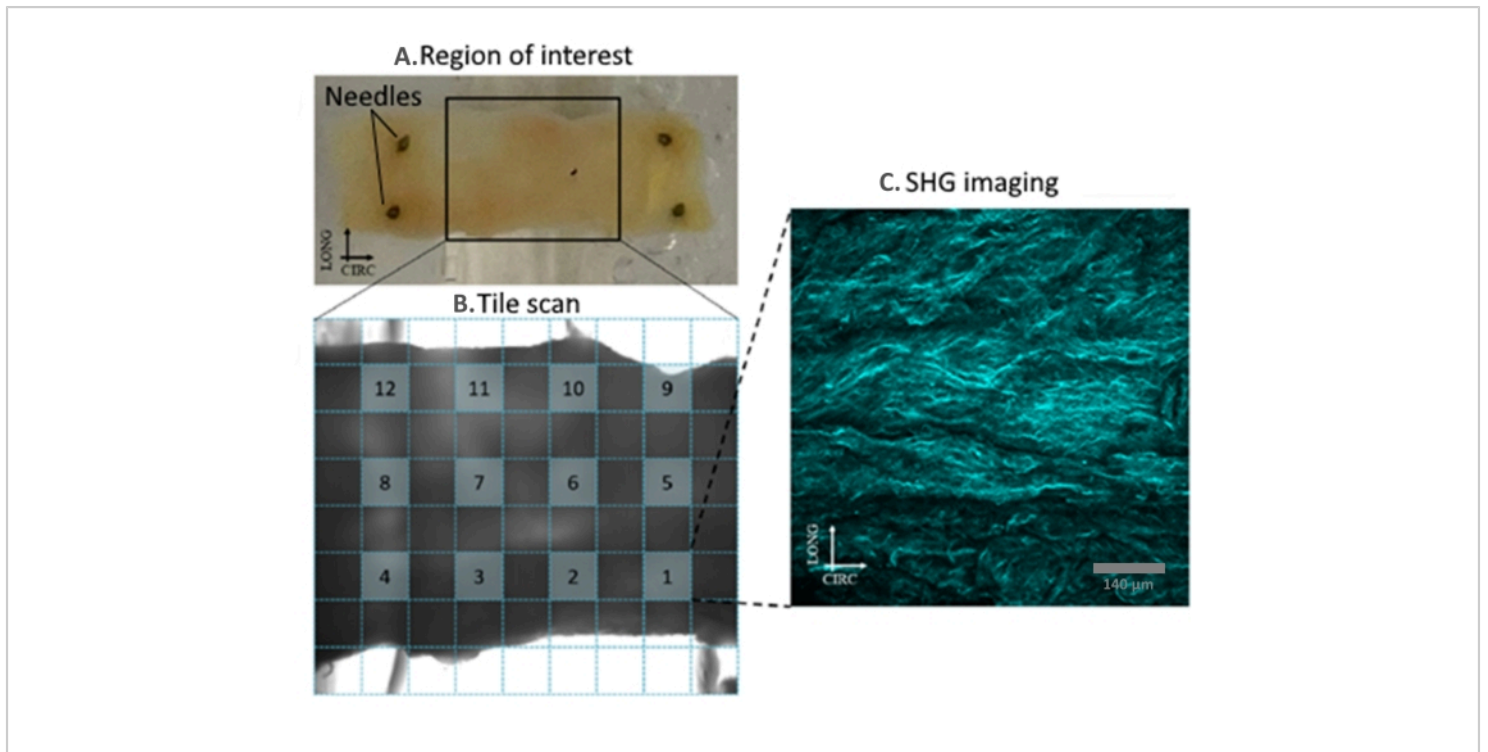
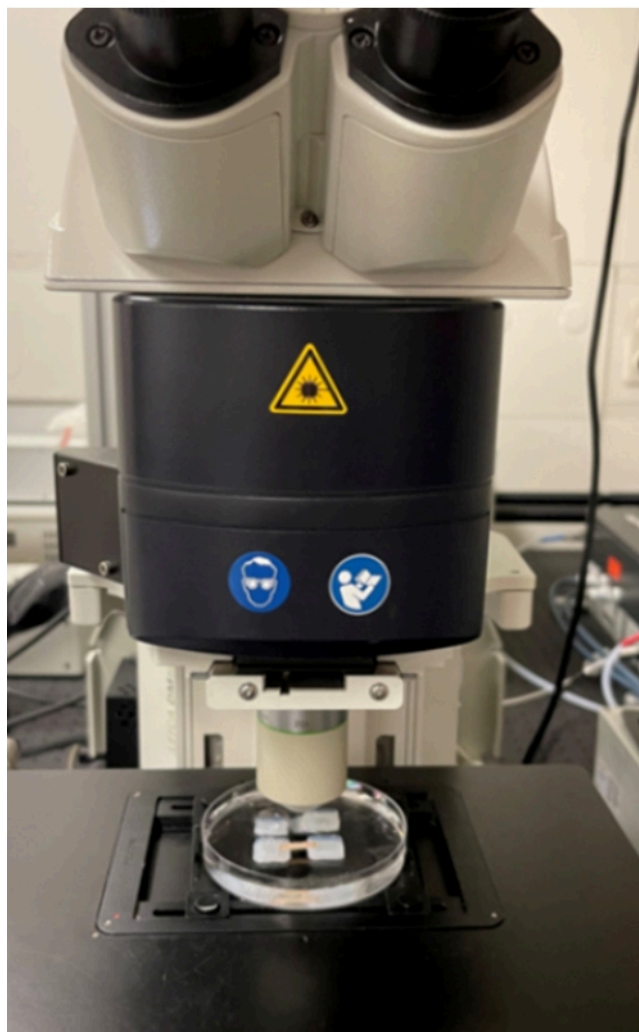


Figure 1: Workflow chart of the presented experimental protocol. [Please click here to view a larger version of this figure.](#)



**Figure 2: Selection of tiles for SHG imaging from the tile scan. (A)** Test sample pinned in silicon. **(B)** Tile scan of the test sample obtained by brightfield microscopy. The tiles that are selected for SHG imaging are marked by blue squares. **(C)** Maximum intensity projection of the MPM with SHG. Scale bar = 140 μm **(C)**. Abbreviations: SHG = second-harmonic generation; MPM = multiphoton microscopy. [Please click here to view a larger version of this figure.](#)



**Figure 3: Plaque sample placed under the objective of the multiphoton microscope.** The location of the plaque sample is secured by a phosphate-buffered saline-filled Petri dish. [Please click here to view a larger version of this figure.](#)

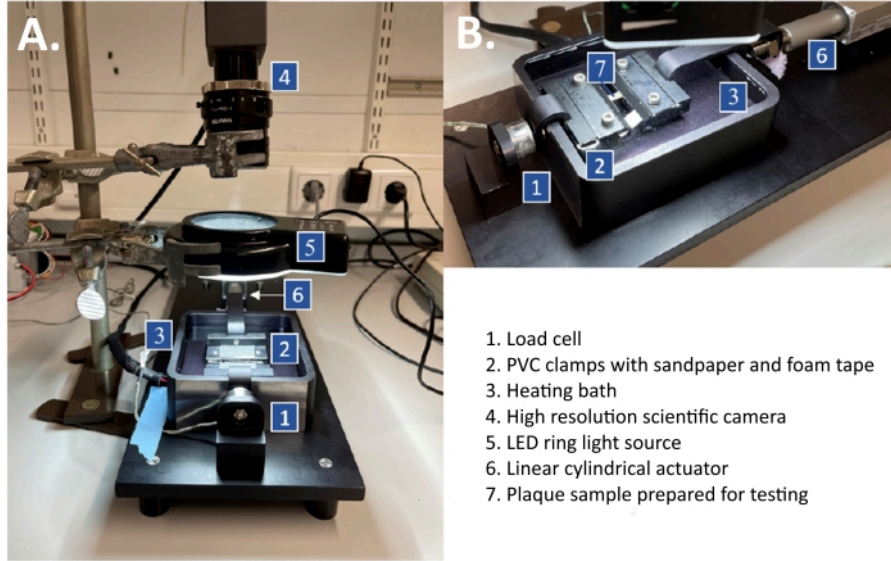


**Figure 4: Custom-designed uniaxial tensile tester with its different components indicated. (A)** Total overview of the system. Note that the sandpaper inserts in the clamps are visible as only the bottom clamps are attached. **(B)** Zoomed-in image of the clamps of the tensile tester with the test specimen ready for testing. Abbreviations: PVC = polyvinyl chloride; LED = light-emitting diode. [Please click here to view a larger version of this figure.](#)



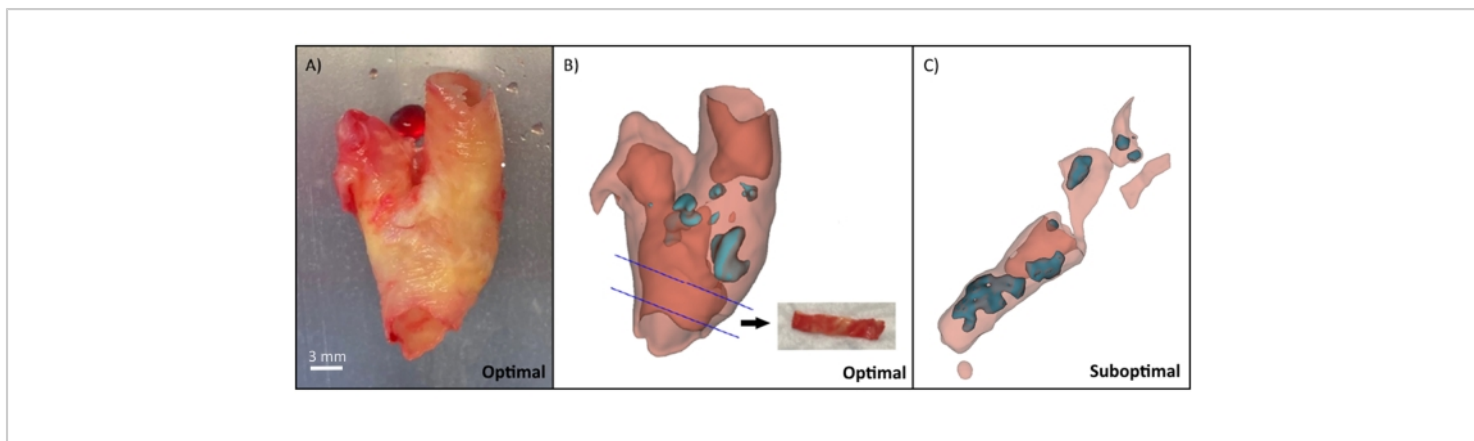


**Figure 5: Tissue collection and sample preparation results from representative samples.** (A) Fresh and intact plaque sample, retrieved from consenting patients who underwent carotid endarterectomy surgery. (B) 3D reconstruction from a  $\mu$ CT scan. Calcified tissue is shown in light blue and non-calcified in red. An optimal sample without calcified tissue could be obtained from the area between the blue lines. (C) 3D reconstruction from the  $\mu$ CT scan showing a suboptimal plaque with an excess of calcified tissue. Scale bar = 3 mm. Abbreviation:  $\mu$ CT = micro-computed tomography. [Please click here to view a larger version of this figure.](#)

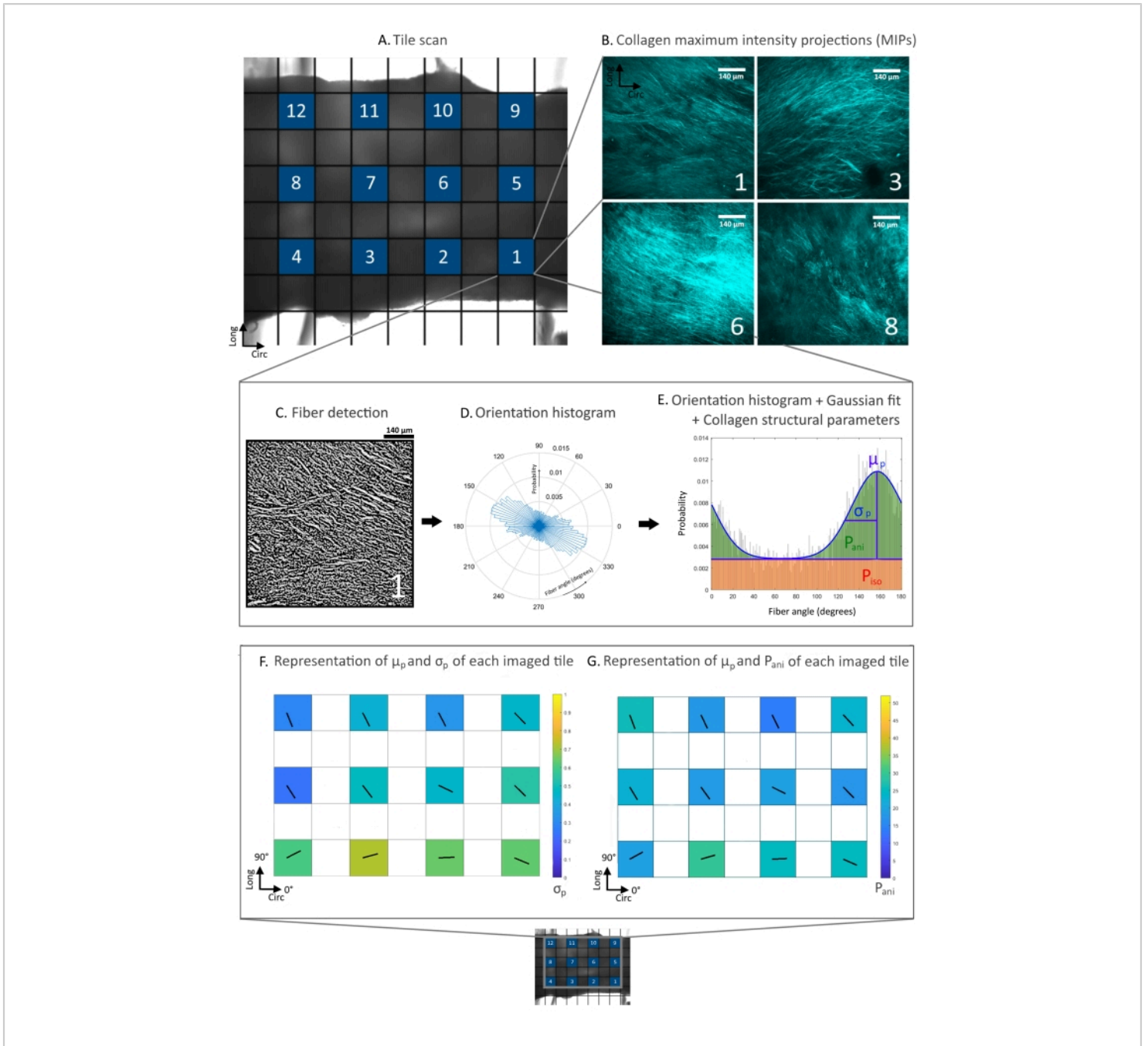


**Figure 6: MPM-SHG results from a representative sample.** (A) Tile scan overview; the selected tiles for imaging are shown in blue. (B) MIPs from various tiles. (C) Fiber detection by the FOA tool from a selected tile (#1). (D) Fiber orientation histogram from a selected tile. (E) Fiber orientation histogram + Gaussian fit, from which collagen structural parameters can be extracted from a selected tile. (F) Representation of the  $\mu_p$  (orientation black line) and  $\sigma_p$  (background color) across the entire plaque sample. (G) Representation of the  $\mu_p$  (orientation black line) and  $P_{ani}$  (background color) across the entire plaque sample. Scale bars = 140  $\mu\text{m}$  (B,C). Abbreviations: MPM-SHG = multiphoton microscopy-second-harmonic generation; MIPs = maximum intensity projections; FOA = fiber orientation analysis;  $\mu_p$  = predominant fiber angle;  $P_{ani}$  =

anisotropic fraction;  $\sigma_p$  = standard deviation of the fiber angle distribution;  $P_{ISO}$  = isotropic fraction. [Please click here to view a larger version of this figure.](#)

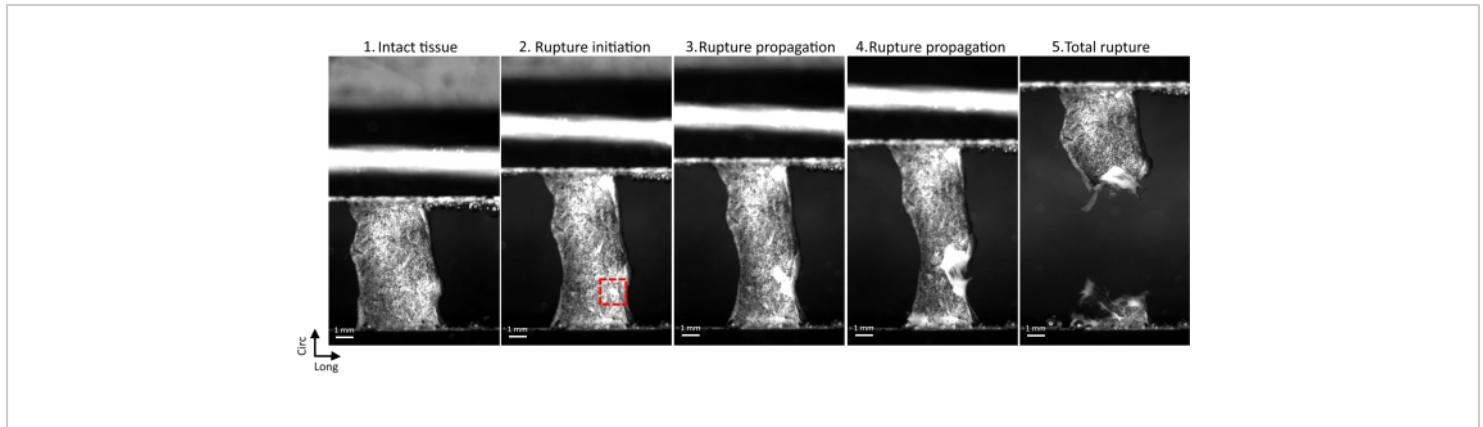


**Figure 7: Rupture initiation and propagation in a plaque tissue sample during the tensile test procedure.1)** Prestretched state, intact tissue. **2)** Rupture initiation-first frame in which rupture is observed. The rupture initiation location is marked with a red square. **3)** and **4)** Rupture propagation. **5)** Complete rupture of the plaque sample. Scale bars = 1 mm. [Please click here to view a larger version of this figure.](#)

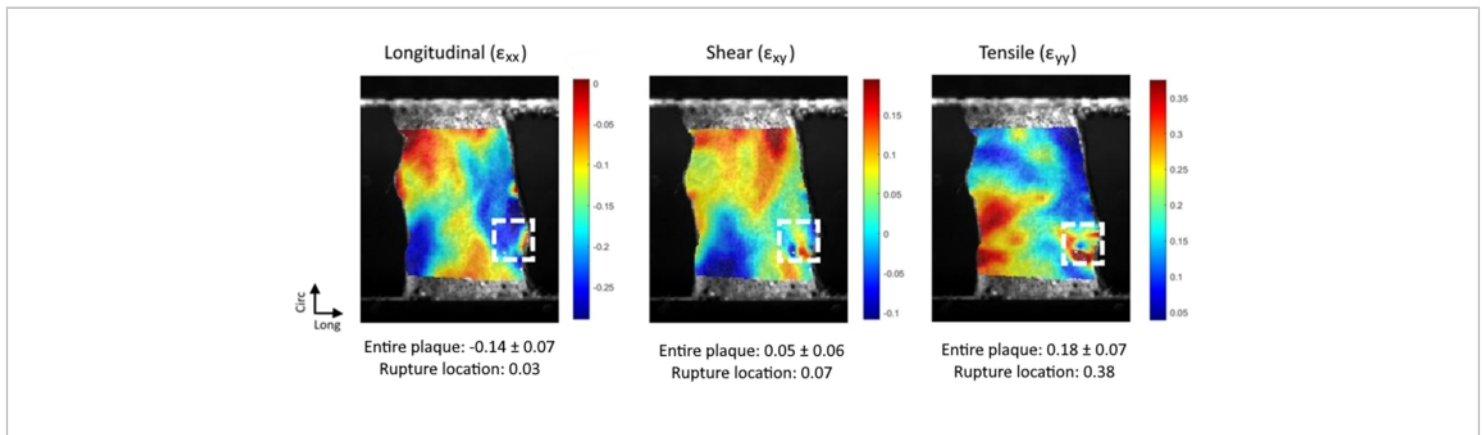


**Figure 8: Green-Lagrange strain patterns of a representative sample ( $\epsilon_{xx}$ ,  $\epsilon_{xy}$ , and  $\epsilon_{yy}$ ) at the frame before rupture, obtained with DIC analysis.** Average and standard deviation over the entire plaque are given, together with the strain at the rupture location. Abbreviations: DIC = digital image correlation;  $\epsilon_{xx}$  = longitudinal strain;  $\epsilon_{xy}$  = shear;  $\epsilon_{yy}$  = tensile strain. [Please click here to view a larger version of this figure.](#)

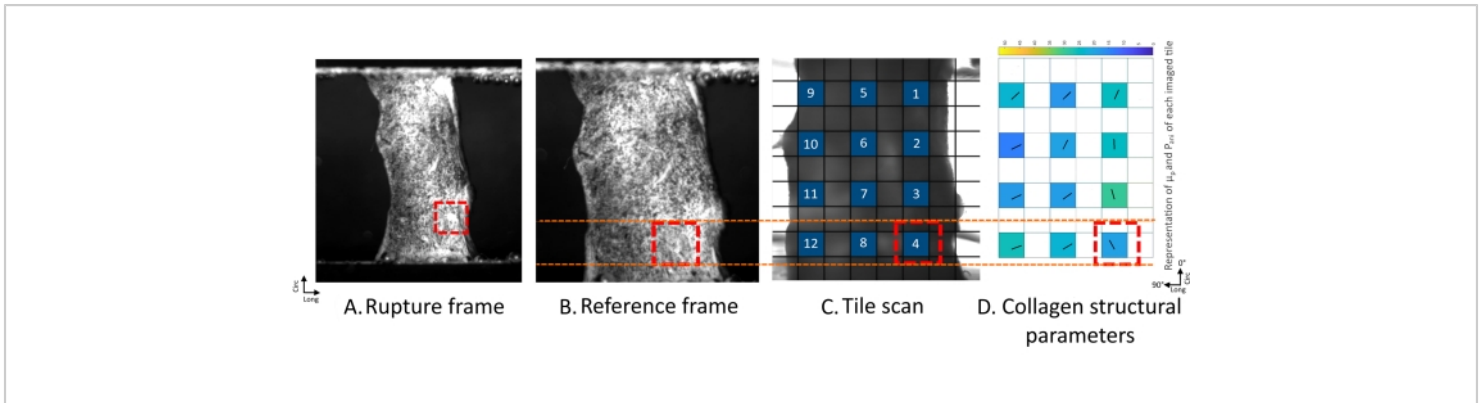


**Figure 9: Overlay image of the rupture location (red square) on images. (A)** High-speed camera image, where rupture is identified (rupture frame). **(B)** High-speed camera image, where only prestretch is applied (reference frame). **(C)** The tile scan image obtained *via* microscopy. **(D)** A color-coded map showing local collagen structural parameters at various tiles. The  $\mu_p$  (orientation black line) and  $P_{ani}$  (background color) across the entire plaque sample are presented. Abbreviations:  $\mu_p$  = predominant fiber angle;  $P_{ani}$  = anisotropic fraction. [Please click here to view a larger version of this figure.](#)

## Discussion

The current study focused on developing a mechano-imaging pipeline to study the correlation between the local collagen orientation and dispersion, local mechanical properties, and rupture behavior of fibrous atherosclerotic plaque tissue. The protocol described herein is innovative for several reasons. First, this is the first time that digital image correlation has been applied to measure the local deformation of fibrous plaque tissue under mechanical loading. Second, this protocol provides the necessary information to analyze the association between the local deformation pattern and the local collagen architecture of the fibrous plaque tissue. The importance of the local assessment is emphasized by both the strain data and the collagen data presented in the results section, which show the heterogeneous nature of the tissue. Therefore, the use of techniques that enable local assessment, such as the ones utilized in this protocol, is recommended for future studies of fibrous plaque properties.

Test sample preparation is among the critical steps of this protocol. Carotid plaques are mainly collagenous tissues; however, they may contain calcifications that are considered to affect the overall plaque mechanical behavior<sup>36,37</sup>. As the study focuses on the fibrous tissue component of the plaque, calcifications are avoided in the test samples by using  $\mu$ CT imaging<sup>38</sup>. If  $\mu$ CT is not available, other imaging techniques such as MRI or OCT<sup>39</sup> can be considered for detecting the calcified regions in the plaque. Obtaining fibrous tissue test samples that are free of calcifications and are of a large enough size that is workable for mechanical testing may be a challenging task for plaques that are heavily calcified or contain dispersed calcifications. Another challenging task in the protocol is generating an optimal speckle pattern for digital image correlation. Optimal DIC requires a black/white ratio of 50:50<sup>28</sup> and speckles the size of three to five pixels<sup>29</sup> to ensure appropriate quality. Failure to meet these requirements may result in inaccurate local strain measurements. Finally, mapping the rupture location to the

SHG images can be challenging if the natural landmarks of a tissue are not clear. For such samples, application of several fiducial markers to the tissue before imaging will be helpful.

The MPM-SHG technique used in the current protocol is superior to many other collagen imaging techniques, as it is a high-resolution and non-destructive technique with a relatively large penetration depth. Yet, the penetration depth (<400  $\mu\text{m}$ ) of MPM-SHG poses a limitation, as it does not allow imaging the entire thickness of the test samples, which ranged between 0.5 and 2 mm. In a recent study with diffusion tensor magnetic resonance imaging (DT-MRI), we have demonstrated that the predominant fiber orientation in the deeper parts of the plaque tissue can be different from the one in the more superficial, luminal parts of the tissue<sup>14</sup>. Therefore, further studies are warranted to investigate the local collagen architecture in the deeper parts of thick fibrous plaque tissue samples and its relation to the local tissue mechanics. For this purpose, polarized spatial frequency domain imaging (pSFDI) can be utilized. This recently developed optical imaging technique was reported to have the potential to measure fiber orientation as deep as 0.8 mm in mitral valve leaflets<sup>12</sup>. The pSFDI also offers a fast acquisition, which could also facilitate visualization of the entire sample area instead of only a selection of tiles, as is the case in the current protocol. Another limitation of the current protocol is that only surface deformation could be identified. In future studies, mirror-assisted multi-view DIC<sup>40</sup> or digital volume correlation (DVC)<sup>41</sup> can be included in this protocol to obtain additional information on the volumetric, subsurface strains.

The current experimental protocol can be further extended or modified in several ways to obtain additional information about plaque rupture mechanics and its relation to the

underlying microstructure. First, the current protocol includes uniaxial tensile testing in the circumferential direction. This type of mechanical testing was chosen since the plaque predominantly experiences tensile stretch in the circumferential direction *in vivo*. For more comprehensive mechanical characterization, this protocol can be further extended to incorporate inflation testing, biaxial testing, or uniaxial tensile testing in the longitudinal direction. Second, the current protocol only focuses on obtaining local strains through DIC. However, a more complete view of the plaque mechanical behavior can be acquired by also including local stress analysis in the protocol, yet this requires characterization of local stiffness. Although currently challenging, this can be achieved by computational techniques such as the inverse finite element method<sup>42,43</sup> and the virtual fields method<sup>44</sup>. Aside from experimental adaptation, some additional postprocessing steps can also be added to the current protocol. First, instead of only identifying the rupture location, the crack-propagation path can be identified *via* the obtained high-speed camera images. This propagation path can be correlated to local structural and mechanical parameters. Second, the rupture initiation location was visually identified in the described protocol. A previous study on non-biological tissues has used discontinuities in DIC strain measurements to detect rupture<sup>45</sup>. Applying such automated rupture detection on plaque tissues can possibly improve the accuracy of the rupture detection. Finally, a great advantage of MPM-SHG compared to other collagen imaging techniques is that it visualizes individual collagen fibers. Therefore, the data obtained *via* this protocol can also be used to investigate additional local collagen characteristics, such as the collagen content.

This protocol can be used to provide a better understanding of the local characteristics of fibrous plaque tissue, the component that mechanically fails in plaque rupture *in vivo*. This information is needed to establish new structural and functional imaging markers that predict plaque rupture in patients. These new markers are necessary, since the previously suggested risk biomarkers have been shown to have suboptimal predictive value for future clinical events<sup>5,6</sup>. In the future, OCT and ps-OCT can possibly identify and quantify fibrous tissue in the arterial system<sup>46,47,48</sup>. In addition, strain was regarded a surrogate marker for local plaque composition<sup>49</sup>. Thus, *in vivo* strain measurements<sup>49</sup> could potentially aid in the identification of plaque stability in patients. However, one should be careful with directly translating the obtained results to *in vivo* plaque rupture. First, the fibrous plaque tissue experiences more complex loading *in vivo* than the unidirectional tensile loading used in this protocol. Second, atherosclerotic plaques are multicomponent structures; the *in vivo* stress and strain distributions in the fibrous plaque tissue can be affected by the presence and location of the other plaque components, such as calcifications<sup>37</sup>.

This mechano-imaging pipeline can also be utilized to study other collagenous tissues. Global mechanical testing and structural imaging of collagen are already widely used for biological tissues. However, local assessment of pre-failure and failure properties, as well as collagen architecture, is critical for accurate mechanical characterization of heterogeneous fibrous tissues. We anticipate that the structure of this new protocol will provide further insight into the interplay between the microstructure and mechanics of several biological tissues.

## Disclosures

The authors have no conflicts of interest to disclose.

## Acknowledgments

This work was funded by an NWO-Vidi grant (18360).

## References

1. Libby, P. et al. Atherosclerosis. *Nature Reviews Disease Primers*. **5** (1), 1-18 (2019).
2. Visseren, F. et al. ESC Guidelines on cardiovascular disease prevention in clinical practice. *European Heart Journal*. **42** (34), 3227-3337 (2021).
3. Jang, I. K. et al. In vivo characterization of coronary atherosclerotic plaque by use of optical coherence tomography. *Circulation*. **111** (12), 1551-1555 (2005).
4. Ohayon, J., et al. Necrotic core thickness and positive arterial remodeling index: emergent biomechanical factors for evaluating the risk of plaque rupture. *American Journal of Physiology. Heart and Circulatory Physiology*. **295** (2), H717-H727 (2008).
5. SCOT-HEART investigators. Coronary CT angiography and 5-year risk of myocardial infarction. *The New England Journal of Medicine*. **379** (10), 924-933 (2018).
6. Williams, M. C. et al. Coronary artery plaque characteristics associated with adverse outcomes in the SCOT-HEART study. *Journal of the American College of Cardiology*. **73** (3), 291-301 (2019).
7. Kwak, B. R. et al. Biomechanical factors in atherosclerosis: mechanisms and clinical implications. *European Heart Journal*. **35** (43), 3013-3020 (2014).

8. Akyildiz, A. C., Speelman, L., Gijssen, F. J. Mechanical properties of human atherosclerotic intima tissue. *Journal of Biomechanics*. **47** (4), 773-783 (2014).
9. Loree, H. M., Grodzinsky, A. J., Park, S. Y., Gibson, L. J., Lee, R.T. Static circumferential tangential modulus of human atherosclerotic tissue. *Journal of Biomechanics*. **27** (2), 195-204 (1994).
10. Holzapfel, G. A., Sommer, G., Regitnig, P. Anisotropic mechanical properties of tissue components in human atherosclerotic plaques. *Journal of Biomechanical Engineering*. **126** (5), 657-665 (2004).
11. Maher, E. et al. Tensile and compressive properties of fresh human carotid atherosclerotic plaques. *Journal of Biomechanics*. **42** (16), 2760-2767 (2009).
12. Teng, Z. et al. A uni-extension study on the ultimate material strength and extreme extensibility of atherosclerotic tissue in human carotid plaques. *Journal of Biomechanics*. **48** (14), 3859-3867 (2015).
13. Lendon, C. L., Davies, M. J., Richardson, P. D., Born, G. V. R. Testing of small connective tissue specimens for the determination of the mechanical behaviour of atherosclerotic plaques. *Journal of Biomedical Engineering*. **15** (1), 27-33 (1993).
14. Akyildiz, A. C., et al. 3D fiber orientation in atherosclerotic carotid plaques. *Journal of Structural Biology*. **200** (1), 28-35 (2017).
15. Johnston, R. D., Gaul, R. T., Lally, C. An investigation into the critical role of fibre orientation in the ultimate tensile strength and stiffness of human carotid plaque caps. *Acta Biomaterialia*. **124**, 291-300 (2021).
16. Larson, A. M. Multiphoton microscopy. *Nature Photonics*. **5** (1), 1 (2010).
17. Pagiatakis, C., Galaz, R., Tardif, J. C., Mongrain, R. A comparison between the principal stress direction and collagen fiber orientation in coronary atherosclerotic plaque fibrous caps. *Medical and Biological Engineering and Computing*. **53** (6), 545-555 (2015).
18. Niestrawska, J. A. et al. The role of tissue remodeling in mechanics and pathogenesis of abdominal aortic aneurysms. *Acta Biomaterialia*. **88**, 149-161 (2019).
19. Woessner, A. E., Jones, J. D., Witt, N. J., Sander, E. A., Quinn, K. P. Three-dimensional quantification of collagen microstructure during tensile mechanical loading of skin. *Frontiers in Bioengineering and Biotechnology*. **9**, 642866 (2021).
20. Kujawinska, M. et al. Digital image correlation method: A versatile tool for engineering and art structures investigations. In *Proceedings of SPIE*. **8011**, 80119R-1 (2011).
21. Luo, Y., Duprey, A., Avril, S., Lu, J. Characteristics of thoracic aortic aneurysm rupture in vitro. *Acta Biomaterialia*. **42**, 286-295 (2016).
22. Bonati, L. H. et al. European Stroke Organisation guideline on endarterectomy and stenting for carotid artery stenosis. *European Stroke Journal*. **6** (2), 1-47 (2021).
23. Hemmasizadeh, A., Darvish, K., Autieri, M. Characterization of changes to the mechanical properties of arteries due to cold storage using nanoindentation tests. *Annals of Biomedical Engineering*. **40** (7), 1434-1442 (2012).
24. Fedorov, A. et al. 3D slicer as an image computing platform for the quantitative imaging network. *Magnetic Resonance Imaging*. **30** (9), 1323-1341 (2012).

25. Mulvihill, J. J., Walsh, M. T. On the mechanical behaviour of carotid artery plaques: the influence of curve-fitting experimental data on numerical model results. *Biomechanics and Modeling in Mechanobiology*. **12** (5), 975-985 (2013).
26. Walsh, M. T. et al. Uniaxial tensile testing approaches for characterisation of atherosclerotic plaques. *Journal of Biomechanics*. **47** (4), 793-804 (2014).
27. Walsh, D. R. et al. Mechanical and structural characterisation of the dural venous sinuses. *Scientific Reports*. **10**, 21763 (2020).
28. Palanca, M., Tozzi, G., Cristofolini, L. The use of digital image correlation in the biomechanical area: a review. *International Biomechanics*. **3** (1), 1-21 (2016).
29. Zhou, P., Goodson, K. E. Subpixel displacement and deformation gradient measurement using digital image/speckle correlation. *Optical Engineering*. **40** (8), 1613-1620 (2001).
30. Frangi, A. F., Niessen, W. J., Vincken, K. L., Viergever, M. A. Multiscale vessel enhancement filtering. *Lecture Notes in Computer Science*. **1496**, .(1998).
31. <https://gitlab.tue.nl/stem/FibLab/-/blob/master/Fibertracking/manual.pdf>. (2016).
32. <https://gitlab.tue.nl/stem/FibLab/-/blob/master/adifferentangle.pdf>. (2021).
33. van Haften, E. et al. Decoupling the effect of shear stress and stretch on tissue growth and remodeling in a vascular graft. *Tissue Engineering Part C: Methods.*, **24** (7), 418-429 (2018).
34. Blaber J., Adair B., Antoniou A. Ncorr: open-source 2D digital image correlation matlab software. *Experimental Mechanics*. **55** (6), 1105-1122 (2015).
35. [http://www.ncorr.com/download/ncorrmanual\\_v1\\_2\\_2.pdf](http://www.ncorr.com/download/ncorrmanual_v1_2_2.pdf). (2017).
36. Barrett, H. E., Van der Heiden, K., Farrell, E., Gijssen, F., Akyildiz, A. C. Calcifications in atherosclerotic plaques and impact on plaque biomechanics. *Journal of Biomechanics*. **87**, 1-12 (2019).
37. Gijssen, F. et al. Morphometric and mechanical analyses of calcifications and fibrous plaque tissue in carotid arteries for plaque rupture risk assessment. *IEEE transactions on Biomedical Engineering*. **68** (4), 1429-1438 (2021).
38. Zhang, L. et al. Advances in CT techniques in vascular calcification. *Frontiers in Cardiovascular Medicine*. **29** (8), 716-822 (2021).
39. Wang, Y., Osborne, M. T., Tung, B., Li, M., Li, Y. Imaging cardiovascular calcification. *Journal of the American Heart Association*. **7** (13), 1-15 (2018).
40. Chen, B., Zhao, J., Pan, B. Mirror-assisted multi-view digital image correlation with improved spatial resolution. *Experimental Mechanics*. **60** (3), 283-293 (2019).
41. Santamaria, V. A. A., Garcia, M. F., Molimard, J., Avril, S. Characterization of chemoelastic effects in arteries using digital volume correlation and optical coherence tomography. *Acta Biomaterialia*. **102**, 127-137 (2019).
42. Guvenir Torun, S. et al. Multicomponent material property characterization of atherosclerotic human carotid arteries through a Bayesian Optimization based inverse finite element approach. *Journal of the Mechanical Behavior of Biomedical Materials*. **126**, 104996 (2022).
43. Guvenir Torun, S. et al. Multicomponent mechanical characterization of atherosclerotic human coronary



arteries: an experimental and computational hybrid approach. *Frontiers in Physiology*. **12**, 733009 (2021).

44. van den Berg, R., Avril S., Gijzen F. J. H., Akyildiz A. C. Material characterization of atherosclerotic plaques with virtual fields method. In *Proceeding Book of 6th International Conference on Computational and Mathematical Biomedical Engineering - CMBE2019*. (2019).
45. Helm, J. D. Digital image correlation for specimens with multiple growing cracks. *Experimental Mechanics*. **48** (6), 753-762 (2008).
46. Nadkarni, S. K. et al. Measurement of collagen and smooth muscle cell content in atherosclerotic plaques using polarization-sensitive optical coherence tomography. *Journal of the American College of Cardiology*. **49** (13), 1474-1481 (2007).
47. Nadkarni, S. K., Bouma, B. E., de Boer, J., Tearney, G. J. Evaluation of collagen in atherosclerotic plaques: the use of two coherent laser-based imaging methods *Lasers in Medical Science*. **24** (3), 439-445 (2009).
48. Villiger, M. et al. Coronary plaque microstructure and composition modify optical polarization: a new endogenous contrast mechanism for optical frequency domain imaging. *Journal of the American College of Cardiology: Cardiovascular Imaging*. **11** (11), 1666-1676 (2018).
49. Schaar, M. D. et al. Characterizing vulnerable plaque features with intravascular elastography. *Circulation*. **108** (21), 2636-2641 (2003).